Investigating one-dimensional diffusion by quasielastic neutron scattering: A theoretical approach

K. Hahn, H. Jobic, and J. Kärger
Fakultät für Physik und Geowissenschaften, Universität Leipzig, Linnéstrasse 5, 04103 Leipzig, Germany, and Institut de Recherches sur la Catalyse, CNRS, 2 Avenue Einstein, 69626 Villeurbanne, France
(Received 22 December 1997)

Scattering functions and full widths at half maximum for quasielastic neutron scattering (QENS) are calculated for diffusion in systems of one-dimensional channels. The self-correlation function for diffusion in isotropically oriented channels is given and it is found that this function diverges at the origin. The calculations are carried out for both normal and single-file diffusion and the influence of the ballistic phase is investigated. It is found that the ballistic phase influences the scattering functions very strongly for large diffusion coefficients. QENS data from the literature are analyzed with respect to this influence. The influence of three different resolution functions (triangular, Gaussian, and Lorentzian) is considered. [S1063-651X(99)11602-7]

PACS number(s): 05.60.−k, 66.30.Dn

I. INTRODUCTION

Diffusion in restricted geometries may substantially differ from diffusion in the bulk phase. Due to the influence of potential walls (i.e., surfaces), the space accessible by the diffusing particles is restricted and the number of available diffusion paths is reduced. Very often, the diffusional behavior is controlled by these surfaces, rather than by the characteristics of the diffusing particles. Such a behavior is found, e.g., in zeolites, where the particles move in systems of channels and pores with diameters in the range of 5 to 10 Å . A special case of diffusion occurs in zeolites with parallel and unconnected channels, where any particle permanently remains in the same channel. This special kind of diffusion is denoted as unidimensional or one-dimensional diffusion. If the particles in a given channel can pass each other, no deviation from the time behavior of normal diffusion will occur and the mean square displacement is proportional to the observation time. However, if the radius of the channel is smaller than the particle diameter, no mutual passages of the particles are possible and a completely different diffusional behavior is expected. In this case, the order of the particles in the channel cannot change. Systems that obey this condition are called single-file systems. Obviously, in such systems, there is a high degree of mutual correlation between the shifts of different particles leading to an essential change in the diffusional behavior. It was found by analytical means [1–3], simulations [4–6], and experiment [7–9] that the mean square displacement in such systems increases in proportion with the square root of observation time that is in contrast to the behavior of normal diffusion also in one-dimensional channels.

Molecular transport in zeolites has been studied by a variety of techniques including adsorption/desorption, permeation, tracer, and spectroscopic methods [10–12,14,15]. It is only by the latter techniques, viz., pulsed-field gradient NMR (PFG NMR) [10,13] and quasielastic neutron scattering (QENS) [14,15], however, that unambiguous information about the time dependence of molecular displacements, and hence of the existence of single-file diffusion, may be obtained. Whereas typical observation times in PFG NMR are a few milliseconds, the accessible time range for QENS is smaller than 10 ns. Therefore, it is interesting to compare results from both methods. Up to now only a few experimental results on single-file diffusion obtained by PFG NMR [7,8] and QENS [9] are published.

II. ONE-DIMENSIONAL DIFFUSION AND SINGLE-FILE DIFFUSION

In the case of one-dimensional normal diffusion the particles can pass each other. There is no substantial change in the diffusional behavior and the mean-square displacement fulfills the Einstein relation

$$\langle z^2 \rangle = 2Dt, \tag{1}$$

where z is the direction of diffusion (channel direction) and D denotes the diffusion coefficient. The diffusion coefficient will decrease if the particle density in the channel increases. A simple jump model [5,10] yields the concentration dependence $D \propto 1-\theta$ with θ denoting the relative occupancy. In the case of single-file diffusion, the mean-square displacement may be represented by a similar relation,

$$\langle z^2 \rangle = 2F\sqrt{t}, \tag{2}$$

where the quantity F as the counterpart of the self-diffusion coefficient is denoted as single-file mobility or simply mobility [5]. This single-file mobility is known to depend still more strongly on the particle density c or the relative occupancy θ than the self-diffusivity, following the relation [1–5]

$$F \propto \frac{1-\theta}{\theta}. \tag{3}$$

Theoretical considerations show that the single-file mobility may be related to the behavior of a sole particle in the channel [3,6]. It is obvious that a sole particle follows Eq. (1) rather than the rules of single-file diffusion [Eq. (2)] because there are no neighboring particles and, therefore, there is no confinement resulting in a deviation from normal diffusion.

One finds [3] that the self-diffusivity D_s of a sole molecule in a channel and the single-file mobility in this channel at a relative occupancy θ are related to each other by the expression

$$D_s = \pi \frac{F^2}{l^2} = \pi \frac{F^2 \theta^2}{(1-\theta)^2 a^2}, \tag{4}$$

where $l = a(1-\theta)/\theta$ denotes the mean-free-path of a particle and a is the particle diameter.

The diffusion coefficient of a single particle D_s as calculated from experimental results for the mobility F via Eq. (4) is known to be very large (e.g., $0.5\times10^{-6}\,\mathrm{m^2\,s^{-1}}$ for tetrafluoromethane in $AlPO_4$-5 [7] or $0.7\times10^{-6}\,\mathrm{m^2\,s^{-1}}$ for methane in ZSM-48 [9]) compared with diffusion coefficients found in three-dimensional zeolites.

The key function controlling the experimental response in both PFG NMR and incoherent QENS is the probability density that a particle, which starts at the origin ($z=0$), is at position z after an evolution time t. In the case of PFG NMR, this function is generally termed the propagator and is denoted by $P(z,t)$. In QENS, the term self-correlation function has been introduced, with the notation $G(z,t)$, which we will use exclusively in the following discussion. In both normal one-dimensional diffusion and single-file diffusion, the self-correlation function is of Gaussian shape [2,3]:

$$G(z,t) = \frac{1}{\sqrt{2\pi\langle z^2\rangle}} \exp\left(-\frac{z^2}{2\langle z^2\rangle}\right). \tag{5}$$

III. MEASURING SELF-DIFFUSION BY QUASIELASTIC NEUTRON SCATTERING

For molecules containing hydrogen, the neutron cross section for incoherent scattering is much larger than for coherent scattering [15]. Therefore, it is possible to measure self-diffusion, i.e., the shifts of individual particles, rather than the evolution of the particle density, which is obtained by coherent scattering.

Throughout this paper we use the quasiclassical approximation for the incoherent scattering function [15]

$$S(\mathbf{Q},\omega) = \frac{1}{2\pi}\int dt \int d\mathbf{r} \exp[i(\mathbf{Q}\mathbf{r}-\omega t)] G(\mathbf{r},t). \tag{6}$$

$\hbar\mathbf{Q}$ describes the momentum transfer, i.e., the difference between outgoing momentum $\hbar\mathbf{k}_{out}$ and incoming momentum $\hbar\mathbf{k}_{in}$, whereas $\hbar\omega$ is the energy transfer in the interaction between neutron beam and diffusing particles.

To obtain the total scattering function the translational part as given in Eq. (6) has to be convoluted with the rotational and vibrational parts. However, since the rotational and vibrational parts involve much larger energy transfers, they are not influenced by the different time behaviors in one-dimensional diffusion; therefore, we neglect these parts here and concentrate on the translational part.

IV. THE SCATTERING FUNCTION FOR DIFFUSION IN A SINGLE CHANNEL

As a first step, we calculate the scattering function for a single channel. For simplicity, it is assumed to be parallel to that of the scattering vector $\mathbf{Q}$. In this case, using Eqs. (5) and (6), the scattering function is found to be

$$S_1(Q,\omega) = \frac{1}{\pi}\int_0^{+\infty} dt \cos(\omega t) \exp\left(-\frac{Q^2\langle z^2\rangle}{2}\right). \tag{7}$$

Inserting the mean-square displacement for normal diffusion [Eq. (1)], the scattering function for normal diffusion is

$$S_1(Q,\omega) = \frac{1}{\pi}\frac{DQ^2}{\omega^2 + (DQ^2)^2}. \tag{8}$$

The scattering function for one-dimensional normal diffusion has a Lorentzian shape as known from three-dimensional diffusion [15]. Alternately, inserting the mean-square displacement for single-file diffusion [Eq. (2)], the scattering function is

$$S_1(Q,\omega) = \frac{x}{\omega}\left[\cos\left(\frac{\pi}{2}x^2\right)\left(\frac{1}{2}-C(x)\right) + \sin\left(\frac{\pi}{2}x^2\right)\left(\frac{1}{2}-S(x)\right)\right], \tag{9}$$

where

$$x = \frac{FQ^2}{\sqrt{2\pi\omega}} \tag{10}$$

and $C(x) \equiv \int_0^x dt \cos(\pi t^2/2)$ and $S(x) \equiv \int_0^x dt \sin(\pi t^2/2)$ denote the Fresnel integrals, following the notation of Ref. [18]. For a numerical evaluation of the scattering function for single-file diffusion, it is useful to introduce the auxiliary function [18]:

$$g(x) = \left[\cos\left(\frac{\pi}{2}x^2\right)\left(\frac{1}{2}-C(x)\right) + \sin\left(\frac{\pi}{2}x^2\right)\left(\frac{1}{2}-S(x)\right)\right]. \tag{11}$$

For $g(x)$, there exists a rational approximation,

$$g(x) = \frac{1}{2+4.142x+3.492x^2+6.670x^3} + \varepsilon(x) \tag{12}$$

with

$$|\varepsilon(x)| \leqslant 2\times10^{-3}. \tag{13}$$

Although $\varepsilon(x)$ seems to be small enough to be neglected, there are some problems when calculating the scattering function around $\omega=0$. Then, the variable x becomes large and for large arguments the auxiliary function becomes small. Therefore, the relative error becomes large and the approximation according to Eq. (12) should be used only as a first estimate.

V. THE SELF-CORRELATION FUNCTION FOR ONE-DIMENSIONAL DIFFUSION IN ISOTROPICALLY ORIENTED CHANNELS

In most experimental circumstances it is not possible to prepare a sample of crystals in such a way that all one-dimensional channels are oriented in the same direction. The common case is that one has to deal with a sample of isotropically oriented channels. Therefore, to compare experimental data with the model, one has to calculate the scattering function $S_3(\mathbf{Q},\omega)$ for diffusion in isotropically oriented channels. This can be obtained either by performing a powder average with the scattering function for one-dimensional diffusion in a single channel or by calculating the scattering function directly from the three-dimensional self-correlation function for isotropically oriented channels. Both methods are equivalent and the only difference is a change in the sequence of the integrations.

Although the scattering function could easily be found by performing the powder averages of Eqs. (8) and (9), we here prefer to calculate the three-dimensional self-correlation functions, because the knowledge of these functions gives some additional insights into the systems under consideration. Furthermore, leaving the integration over the observation time as the last step will also allow the possibility to examine other time dependencies than those given by Eqs. (1) and (2).

Let $G_1(z,t)$ be the self-correlation function of a diffusing particle in a single one-dimensional channel. This self-correlation function describes the probability density that a particle starting at the origin is at position z after a time interval t. The three-dimensional self-correlation function $G_3(\mathbf{r},t)$ is then the combined probability density that a channel goes through the point $\mathbf{r}$ and that the particle has a displacement $r=|\mathbf{r}|$. The latter probability is simply given by the one-dimensional self-correlation function $G_1(z=r=|\mathbf{r}|,t)$. The probability density to find a given channel on the surface of a sphere with radius r is $(2\pi r^2)^{-1}$. The proportionality with r^{-2} reflects the fact that the number of channels is constant and, therefore, that the probability to find a given channel in a certain area is the inverse of the total surface of the sphere. An additional factor 1/2 arises because a given channel found on the surface at $\mathbf{r}$ is also found at $-\mathbf{r}$. Combining the two probabilities, the three-dimensional self-correlation function for isotropically distributed channels is found to be

$$G_3(\mathbf{r},t)=\frac{1}{2\pi r^2}G_1(r,t). \tag{14}$$

In all relevant cases to be considered here the self-correlation function in a single channel is a Gaussian [Eq. (5)]. With Eq. (14), the three-dimensional self-correlation function of the system of channels hence results to be

$$G_3(\mathbf{r},t)=\frac{1}{(2\pi)^{3/2}\langle z^2\rangle^{1/2}r^2}\exp\left(-\frac{r^2}{2\langle z^2\rangle}\right). \tag{15}$$

In Eq. (15) the mean-square displacement $\langle z^2\rangle$ is that of a single channel, i.e., that of the self-correlation function (5). Determining the mean-square displacement $\langle r^2\rangle = \int_{-\infty}^{\infty} d\mathbf{r} r^2 G_3(\mathbf{r},t)$ for the system of isotropically oriented channels, it is found that $\langle r^2\rangle = \langle z^2\rangle$. This is in contrast to three-dimensional normal diffusion, where the mean-square displacement for three dimensions is three times the mean-square displacement of a selected single dimension ($\langle r^2\rangle = \langle x^2\rangle + \langle y^2\rangle + \langle z^2\rangle$). From now on, we will write σ^2 for the mean-square displacement $\langle r^2\rangle$.

It is remarkable that the self-correlation function $G_3(\mathbf{r},t)$ is no longer a Gaussian. Now, in the denominator there occurs a factor r^2, which leads to a discontinuity at $r=0$. The probability of finding a particle around $r=0$ is much larger than in the case of a Gaussian distribution, whereas the probability of finding a particle at large r is much smaller. Therefore, in this case, the particles are much more concentrated around the origin than in the case of conventional three-dimensional diffusion, which is described by a Gaussian self-correlation function. This concentration is the consequence of the higher probability to find a specific channel on a certain area of a surface with small radius r compared with surfaces with large radius.

VI. THE SCATTERING FUNCTION FOR ONE-DIMENSIONAL DIFFUSION IN ISOTROPICALLY ORIENTED CHANNELS

Once the self-correlation function for isotropically oriented channels is known, the scattering function is found from Eq. (6) as

$$S_3(\mathbf{Q},\omega)=\frac{1}{2\pi}\int dt\int d\mathbf{r}\exp(-i\omega t)\exp(i\mathbf{Q}\mathbf{r})G_3(\mathbf{r},t) \tag{16}$$

$$=\frac{1}{\pi}\int_0^\infty dt\int_0^\infty dr\int_0^{2\pi}d\varphi\int_0^{\pi}d\theta r^2\sin(\theta)\cos(\omega t)\times\cos[Qr\cos(\theta)]\frac{1}{2\pi r^2}G_1(r,t), \tag{17}$$

where Eq. (14) was used to substitute $G_3(\mathbf{r},t)$ and the one-dimensional self-correlation function $G_1(r,t)$ was assumed to be an even function in both r and t. Performing the integration over φ and substituting $\cos(\theta)\equiv s$, the scattering function becomes

$$S_3(\mathbf{Q},\omega)=\frac{2}{\pi}\int_0^\infty dt\int_0^\infty dr\int_0^1 ds\cos(\omega t)\cos(Qrs)G_1(r,t). \tag{18}$$

Assuming a Gaussian shape for the self-correlation function $G_1(r,t)$, the integrals over r and s can be calculated, resulting in the scattering function

$$S_3(\mathbf{Q},\omega)=\frac{1}{\sqrt{2\pi}}\int_0^\infty dt\frac{1}{Q\sigma}\cos(\omega t)\,\mathrm{erf}\left(\frac{Q\sigma}{\sqrt{2}}\right), \tag{19}$$

where $\mathrm{erf}(x)=(2/\sqrt{\pi})\int_0^x dt e^{-t^2}$ denotes the error function. For normal diffusion, where the mean-square displacement behaves as $\sigma^2=\langle r^2\rangle=2Dt$, the solution is known to be [16]

$$S_3(Q,\omega)=\frac{1}{4\pi\sqrt{2}\,y\omega}\left[\ln\left(\frac{1+y^2-y\sqrt{2}}{1+y^2+y\sqrt{2}}\right)+2\arctan(1+\sqrt{2}y)-2\arctan(1-\sqrt{2}y)\right] \tag{20}$$

with

$$y=\frac{\sqrt{D}Q}{\sqrt{\omega}}. \tag{21}$$

For $\omega=0$ the scattering function in Eq. (20) diverges, regardless of the momentum transfer Q. This behavior at $\omega=0$ (and thus for large time scales) is different from normal three-dimensional diffusion, where the scattering function diverges only if momentum and energy transfer vanish simultaneously. The different behavior of these two cases is an immediate consequence of the corresponding self-correlation functions. In the case of normal three-dimensional diffusion, the probability that a particle has moved over a finite nonvanishing distance in a long time interval is large and thus an energy transfer occurs. Otherwise, in the case of diffusion in isotropically oriented channels, the probability that a particle is near $r=0$ is large also for long time intervals. But, if no particle shift occurs, there is no energy transfer and due to the discontinuity in the self-correlation function $G_3(\mathbf{r},t)$ at $r=0$ [see Eq. (15)], a discontinuity in the scattering function at $\omega=0$ arises [17].

By setting $\omega=0$ in Eq. (19), it may be shown that this behavior not only results for normal one-dimensional diffusion, but for all processes where for, $t\to\infty$, the mean-square displacement behaves as $\sigma^2=\langle r^2\rangle\propto t^\alpha$ with $\alpha<2$. Therefore, the discontinuity arises for any realistic time behavior of the diffusional process in isotropically oriented channels, especially for normal ($\alpha=1$) and single-file ($\alpha=0.5$) diffusion.

VII. THE INFLUENCE OF THE EXPERIMENTAL RESOLUTION ON THE SCATTERING FUNCTION

The discontinuity in Eq. (19) does not directly appear in the experimental data because the incoming neutron beam is never strictly monochromatic with a fixed incoming energy ω_{in}. In reality, there is a more or less sharp energy distribution around ω_{in}, which is described by the energy resolution function $R(\hat{\omega}_{in},\omega_{in},\delta)$. This function gives the probability that a neutron of the incoming beam has the energy $\hbar\hat{\omega}_{in}$, when the mean energy is $\hbar\omega_{in}$. The parameter δ describes the width of the resolution function.

The scattering function given by Eq. (19) has to be convoluted, therefore, with the energy resolution function $R(\hat{\omega}-\omega,\delta)$,

$$S_{3,R}(\mathbf{Q},\omega,\delta)=\frac{1}{\sqrt{2\pi}}\int_{-\infty}^{\infty}d\hat{\omega}\int_0^\infty dtR(\hat{\omega}-\omega,\delta)\times\frac{1}{Q\sigma}\cos(\hat{\omega}t)\,\mathrm{erf}\left(\frac{Q\sigma}{\sqrt{2}}\right). \tag{22}$$

Introducing the auxiliary function

$$H(t,\omega,\delta)=\int_{-\infty}^{\infty}d\hat{\omega}R(\hat{\omega}-\omega,\delta)\cos(\hat{\omega}t), \tag{23}$$

which is proportional to the cosine Fourier transform of the energy resolution function, the scattering function becomes

$$S_{3,R}(\mathbf{Q},\omega,\delta)=\frac{1}{\sqrt{2\pi}}\int_0^\infty dtH(t,\omega,\delta)\frac{1}{Q\sigma}\,\mathrm{erf}\left(\frac{Q\sigma}{\sqrt{2}}\right). \tag{24}$$

In most cases the energy distribution function or resolution is a function with a narrow peak at $\hat{\omega}=\omega$. In this paper we restrict ourselves to the three most prominent representations, viz., a triangular resolution:

$$R(\hat{\omega}-\omega,\delta)=\begin{cases}\frac{1}{\delta^2}(\hat{\omega}-\omega+\delta), & \omega-\delta\leqslant\hat{\omega}\leqslant\omega\\ \frac{1}{\delta^2}(-\hat{\omega}+\omega+\delta), & \omega\leqslant\hat{\omega}\leqslant\omega+\delta\\ 0, \quad \text{else,}\end{cases} \tag{25}$$

Gaussian resolution:

$$R(\hat{\omega}-\omega,\delta)=\frac{1}{\sqrt{2\pi}\delta}\exp\left(-\frac{(\hat{\omega}-\omega)^2}{2\delta^2}\right), \tag{26}$$

and Lorentzian resolution:

$$R(\hat{\omega}-\omega,\delta)=\frac{1}{\pi}\,\frac{\delta}{\delta^2+(\hat{\omega}-\omega)^2}. \tag{27}$$

The triangular resolution applies to the neutron spectrometer, which was used in the experiment described in Ref. [9] (IN5), where a narrow energy distribution is selected from a white beam using multichoppers.

The corresponding auxiliary functions are

$$H(t,\omega,\delta)=\frac{4}{\delta^2t^2}\cos(\omega t)\sin^2\left(\frac{\delta t}{2}\right) \tag{28}$$

for triangular resolution,

$$H(t,\omega,\delta)=\cos(\omega t)\exp\left(-\frac{t^2\delta^2}{2}\right) \tag{29}$$

for Gaussian resolution, and

$$H(t,\omega,\delta)=\cos(\omega t)\exp(t\delta) \tag{30}$$

for Lorentzian resolution.

Inserting the auxiliary function from Eq. (28) into Eq. (24) we finally have for the scattering function with triangular resolution, e.g.,

$$S_{3,R}(\mathbf{Q},\omega,\delta)=2\frac{\sqrt{2}}{\sqrt{\pi}}\int_0^\infty dt\frac{1}{Q\sigma}\frac{1}{\delta^2t^2}\times\cos(\omega t)\sin^2\left(\frac{\delta t}{2}\right)\mathrm{erf}\left(\frac{Q\sigma}{\sqrt{2}}\right). \quad (31)$$

This equation holds true for any time behavior of the mean-square displacement σ^2.

In the following, we will use the quite general notation,

$$\sigma^2=2dt^{2\mu} \quad (32)$$

including the cases of normal diffusion (with $\mu=1/2$ and $d=D$) and single-file diffusion (with $\mu=1/4$ and $d=F$).

Although no analytical solution of the integral in Eq. (24) with the time behavior of Eq. (32) is known, an estimate for large values of $Q\sqrt{d}$ can be given. In this case, the argument of the error function $\mathrm{erf}(Q\sqrt{d}t^\mu)$ is large and the error function approaches 1 already for short times t. Therefore, the error function can be omitted for large $Q\sqrt{d}$ in Eq. (31). For the resulting integrals analytical solutions are known:

$$S_{3,R}(\mathbf{Q}\to\infty,\omega,\delta)=\frac{1}{8}\frac{1}{2^\mu}\frac{1}{Q\sqrt{d}\delta^2}\frac{\Gamma\left(-\frac{1+\mu}{2}\right)}{\Gamma\left(\frac{2+\mu}{2}\right)}\times[2\omega^{1+\mu}-(|\omega+\delta|)^{1+\mu}-(|\omega-\delta|)^{1+\mu}] \quad (33)$$

for triangular resolution,

$$S_{3,R}(\mathbf{Q}\to\infty,\omega,\delta)=\frac{1}{4\sqrt{\pi}Q\sqrt{d}}\left(\frac{\delta^2}{2}\right)^{-(1-\mu)/2}\times\Gamma\left(\frac{1-\mu}{2}\right)\,{}_1F_1\left(\frac{1-\mu}{2};\frac{1}{2};-\frac{\omega^2}{2\delta^2}\right) \quad (34)$$

for Gaussian resolution, and

$$S_{3,R}(\mathbf{Q}\to\infty,\omega,\delta)=\frac{1}{2\sqrt{\pi}Q\sqrt{d}}\Gamma(1-\mu)(\omega^2+\delta^2)^{-(1-\mu)/2}\times\cos\left[(1-\mu)\arctan\left(\frac{\omega}{\delta}\right)\right] \quad (35)$$

for Lorentzian resolution. The function ${}_1F_1(a;b;x)$ denotes the confluent hypergeometric function [18] [alternative notations for this function are $\Phi(a;b;x)$ or $M(a,b,x)$].

Once the scattering function is known, the full width at half maximum (FWHM) can be found from the relation

$$S_{3,R}\left(\mathbf{Q},\frac{\Delta\omega}{2},\delta\right)=\frac{1}{2}S_{3,R}(\mathbf{Q},0,\delta), \quad (36)$$

where $\Delta\omega$ denotes the FWHM. Now we consider $\Delta\omega$ as a function of μ. In order to have a generalized width, which is independent of δ, we introduce the new variable

$$\Delta\Omega=\frac{\Delta\omega(\mu)}{\Delta\omega_0}, \quad (37)$$

where $\Delta\omega_0$ denotes the width at $\mu=0$.

Generally, it can be shown by analytical means that the scattering function (Eq. 24) is identical to the resolution function $R(\omega,\delta)$ when $Q\sqrt{d}=0$. This condition is fulfilled if either $\mu=0$ or $Q=0$ and, therefore, in both cases we have $S_{3,R}(Q,\omega,\delta)=R(\omega,0,\delta)$. This can be rationalized by the fact that at $\mu=0$, the particles do not move and, therefore, there is only pure elastic scattering. Thus, the outgoing energy distribution is the same as the incoming distribution. The same is true for the energy distribution at $Q=0$. In this case there is neither a momentum nor an energy transfer and again incoming and outgoing energy distributions are the same. Then, in both cases ($\mu=0$ and $Q=0$), the width $\Delta\omega_0$ of the scattering function is the same as the width of the resolution function. In the cases under consideration, this quantity, expressed as a function of δ, is

$$\Delta\omega_0=\delta \quad (38)$$

for triangular resolution,

$$\Delta\omega_0=2\sqrt{2\ln(2)}\,\delta \quad (39)$$

for Gaussian resolution, and

$$\Delta\omega_0=2\delta \quad (40)$$

for Lorentzian resolution.

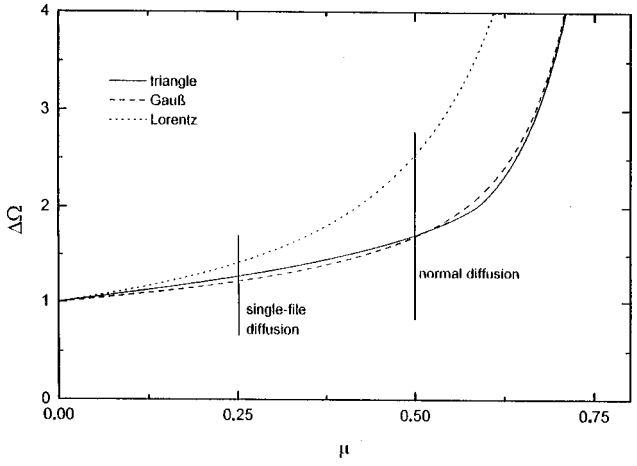

FIG. 1. The width $\Delta\Omega$ at $Q\to\infty$ as a function of the exponent μ for triangular, Gaussian, and Lorentzian resolution.

TABLE I. The relative full width at half maximum $\Delta\Omega$ at $Q \rightarrow \infty$ for single-file and normal diffusion in isotropically oriented channels.

	Single-file $\mu = 0.25$	Normal $\mu = 0.5$
Triangular	1.2687	1.7108
Gaussian	1.2145	1.6968
Lorentzian	1.4124	2.5425

The width $\Delta\Omega$ at $Q \rightarrow \infty$ as a function of the exponent μ is given in Fig. 1. While for $\mu < 0.6$ the width grows slowly from δ to 2δ, for $\mu > 0.6$ there is a very steep ascent leading to $y \rightarrow \infty$ at $\mu = 1$. It should be noted here that the FWHM for $Q \rightarrow \infty$ is finite in all cases with $\mu < 1$. This is in striking contrast to three-dimensional normal diffusion where the width for large Q is proportional to Q and thus goes to infinity.

For the cases of normal ($\mu = 0.5$) and single-file ($\mu = 0.25$) diffusion, the widths $\Delta\Omega$ for the different resolution functions are given in Table I. Whereas the values for Gaussian and triangular resolution are very similar, the width for Lorentzian resolution is much larger.

For $\mu \rightarrow 1$, the integral in Eq. (31) is dominated by the behavior of the integrand at $t \rightarrow 0$ and, thus, the approximation erf$\rightarrow 1$ is not good in this region. Therefore, the FWHM as predicted from Eqs. (33), (34), and (35) in Fig. 1 will be reached only at very large $Q\sqrt{d}$. For diffusion processes, where the exponent $\mu \leqslant 0.5$, the approximation should be good enough and the FWHM reaches its maximum value already at intermediate values of $Q\sqrt{d}$.

The behavior of the FWHM for triangular resolution as a function of the momentum transfer Q for normal and single-file diffusion in isotropically oriented channels as resulting from numerical evaluation of Eq. (31) is given in Figs. 2 and 3, respectively. For the width δ of the resolution function, a value of 0.018 meV is used. This is the same value as used in a recent experiment on IN5 [9]. In the experimentally accessible range of $Q = 0.1$–2.0 Å^{-1} diffusivities D larger than 1×10^{-6} m^2 s^{-1} cannot be distinguished by comparing the FWHM, because for diffusivities larger than this limit, the FWHM has reached its maximum value already at $Q = 0.2$ Å^{-1} (see Fig. 2). In the single-file case the limit is at a mobility of $F = 1 \times 10^{-12}$ m^2 s$^{-1/2}$ (see Fig. 3). The behavior of the FWHM in the cases of Gaussian and Lorentzian resolution is similar and the limiting diffusivities or mobilities are of the same order as in the case of triangular resolution.

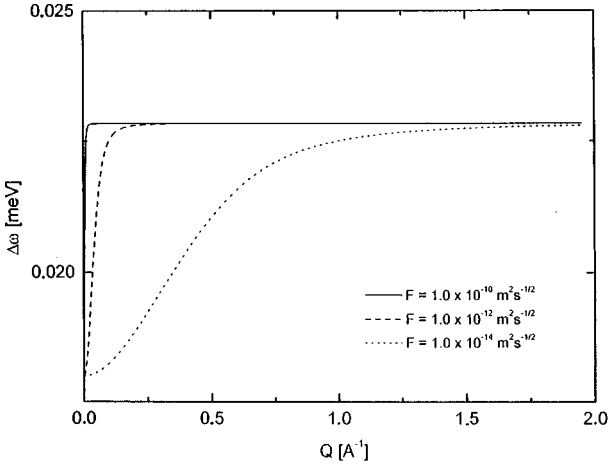

FIG. 3. The width $\Delta\omega$ for single-file diffusion with triangular resolution as a function of the momentum transfer Q for different mobilities.

Whereas the determination of diffusion coefficients or mobilities using the FWHM is not always possible, these quantities can be found using the scattering functions. In Figs. 4 and 5 the scattering functions with triangular resolution for three-dimensional normal diffusion and for normal and single-file diffusion in isotropically oriented channels at a momentum transfer of $Q = 0.35$ Å^{-1} are compared. The relevant parameters (diffusivities and mobilities, respectively) are chosen in such a way that the other amplitudes are best fits to the scattering amplitude of normal diffusion in channels. For very small parameters (Fig. 4) the scattering functions are almost identical and it is impossible to distinguish between the three different types of diffusional behavior. The shape is essentially governed by the instrumental

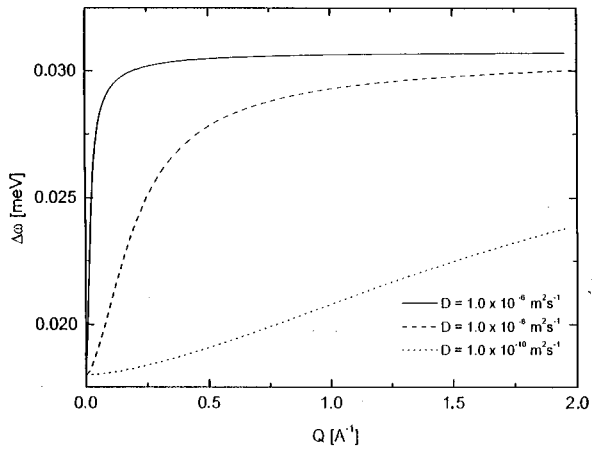

FIG. 2. The width $\Delta\omega$ for normal diffusion with triangular resolution as a function of the momentum transfer Q for different diffusivities.

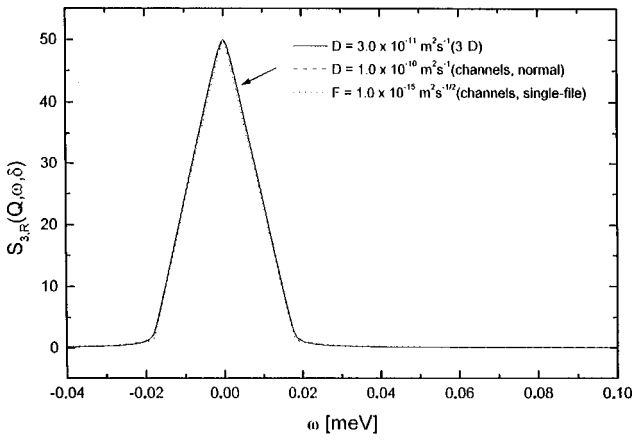

FIG. 4. The scattering function $S_{3,R}(Q,\omega,\delta)$ for three-dimensional normal diffusion and for normal and single-file diffusion in isotropically oriented channels at $Q = 0.35$ Å^{-1} (triangular resolution). Small diffusion coefficients.

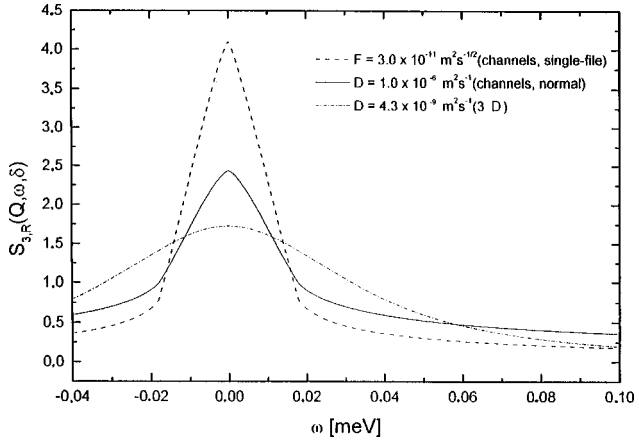

FIG. 5. The scattering function $S_{3,R}(Q,\omega,\delta)$ for three-dimensional normal diffusion and for normal and single-file diffusion in isotropically oriented channels at $Q=0.35$ Å^{-1} (triangular resolution). Large diffusion coefficients.

resolution. Only the scattering function for single-file diffusion differs slightly from the other ones around $\omega=0.02$ meV. Experimentally, this means that one would have to resort to another spectrometer having a higher resolution. For larger parameters (Fig. 5) the scattering functions are well separated and both the determination of the principal diffusional behavior and the diffusivity or mobility can easily be done.

As an example, we compare the theoretical scattering functions with experimental data, found for methane in the zeolite ZSM-48 (for details see Ref. [9]). The data are given for a momentum transfer of $Q=0.35$ Å^{-1}, where the influence of rotation is small and can be neglected. In Fig. 6 the data together with the best fits to the experimental data for normal and single-file diffusion in isotropically oriented channels are given. The fits were carried out minimizing the function

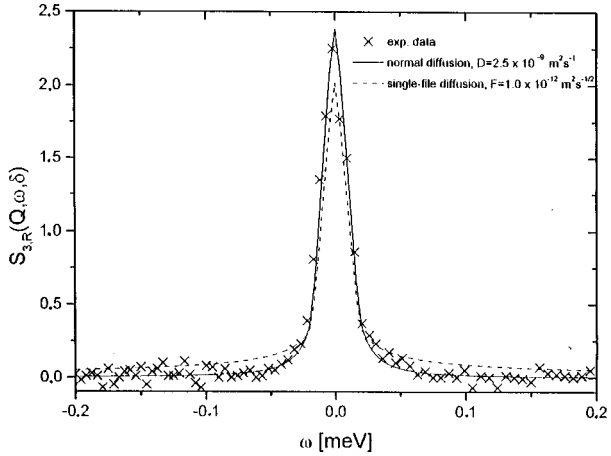

FIG. 6. Comparison of experimental data from the diffusion of methane in ZSM-48 with the scattering functions for normal and single-file diffusion in isotropically oriented channels at $Q=0.35$ Å^{-1}.

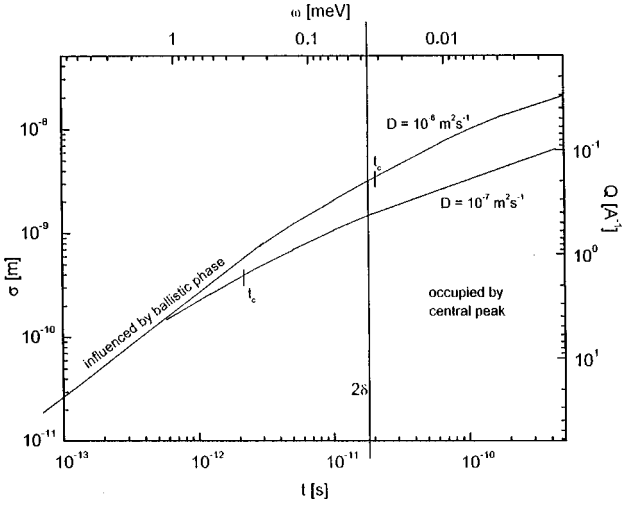

FIG. 7. The space and time ranges (left and lower axis) together with the corresponding ranges of momentum and energy transfer (right and upper axis) relevant for QENS. The vertical straight line divides the plane into the range occupied by the central peak of the scattering function for the case without ballistic phase (right-hand side) and into the range not occupied by the central peak (left-hand side). The mean shift σ for normal diffusion with initial ballistic phase is given for two diffusivities ($D=10^{-6}$ and 10^{-7} m^2/s).

$$R_{\mathrm{wp}}=\left(\frac{\sum_i w_i[y_i(\mathrm{obs})-y_i(\mathrm{calc})]^2}{\sum_i w_i y_i^2(\mathrm{obs})}\right)^{1/2}, \qquad (41)$$

where y_i(obs) and y_i(calc) denote the experimental and theoretical values of the scattering functions, respectively, and the weight is $w_i=1/y_i$(obs). Whereas the scattering function for normal diffusion with $D=2.5\times10^{-9}$ m^2 s^{-1} reproduces the data very well ($R_{\mathrm{wp}}=12.4$), the function for single-file diffusion does not fit to the data ($R_{\mathrm{wp}}=18.9$). It is not possible to reproduce the experimental data with the single-file diffusion function both in the central peak and in the wings.

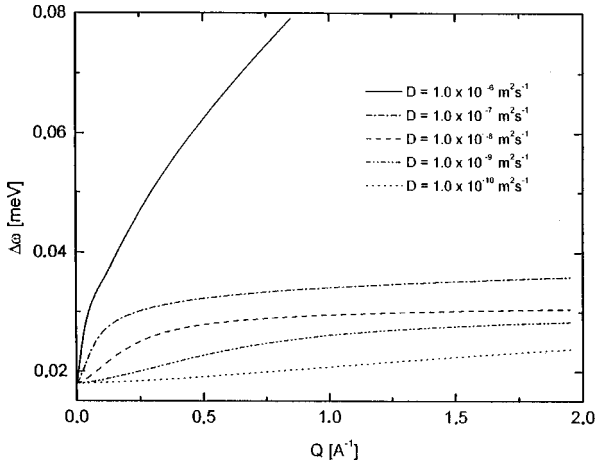

FIG. 8. The width $\Delta\omega$ for normal diffusion with triangular resolution as a function of the momentum transfer Q for different diffusivities. A ballistic phase with a velocity of $v=280$ m/s is assumed.

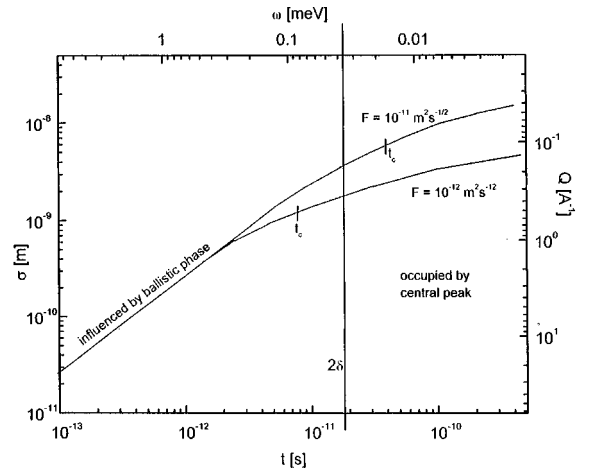

FIG. 9. The space and time ranges (left and lower axis) together with the corresponding ranges of momentum and energy transfer (right and upper axis) relevant for QENS. The vertical straight line divides the plane into the range occupied by the central peak of the scattering function for the case without ballistic phase (right-hand side) and into the range not occupied by the central peak (left-hand side). The mean shift σ for single-file diffusion with initial ballistic phase is given for two mobilities ($F=10^{-11}$ and 10^{-12} $\mathrm{m^2/s^{1/2}}$).

VIII. THE INFLUENCE OF THE BALLISTIC PHASE ON THE SCATTERING FUNCTION

Quasielastic neutron scattering measures the behavior of a system on a time scale of 10^{-12} to 10^{-8} s. These times are very short compared with the range accessible by PFG NMR and it is not obvious whether the long-time behavior is already established in the QENS measurements. At short times the behavior of the particles is ballistic, i.e., $\langle z^2\rangle = v^2t^2$, and there exists a transition time t_c where the system behavior switches from the ballistic phase to normal or single-file diffusion. We define the transition time t_c as the crossover time of the two asymptotic behaviors, i.e., the time when the mean square displacements of the two processes are the same,

$$\sigma^2 = v^2t_c^2 = 2dt_c^{2\mu}. \tag{42}$$

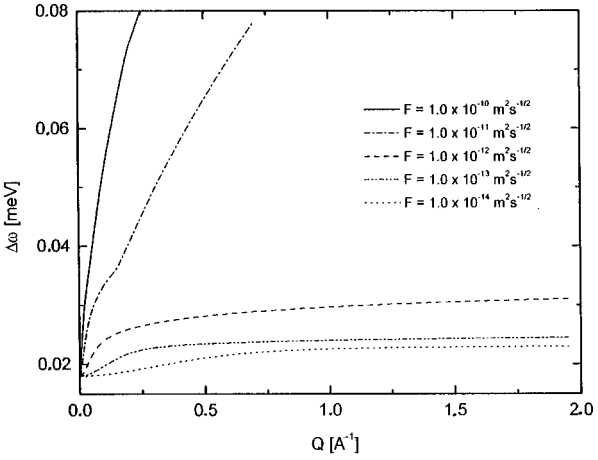

FIG. 10. The width $\Delta\omega$ for single-file diffusion with triangular resolution as a function of the momentum transfer Q for different mobilities. A ballistic phase with a velocity of $v=280$ m/s is assumed.

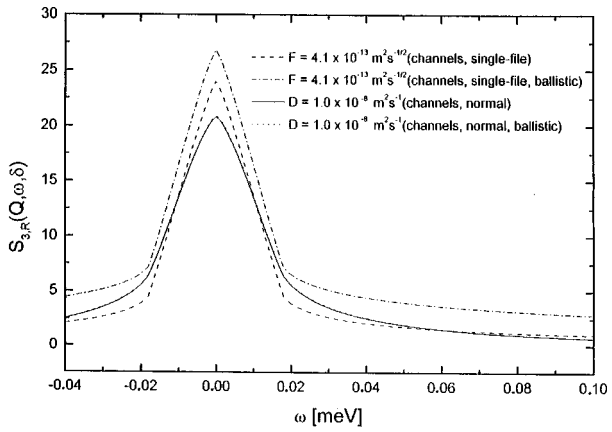

FIG. 11. The scattering function $S_{3,R}(Q,\omega,\delta)$ for three-dimensional normal diffusion and for normal and single-file diffusion with and without ballistic phase in isotropically oriented channels at $Q=0.35$ Å^{-1} (triangular resolution). Diffusivity and mobility chosen such that ranges influenced by ballistic phase and occupied by central peak do not overlap.

We thus obtain

$$t_c = \left(\frac{2d}{v^2}\right)^{1/(2-2\mu)}. \tag{43}$$

The velocity v during the ballistic phase coincides with the thermal velocity of the particles

$$v = \left(\frac{kT}{m}\right)^{1/2}, \tag{44}$$

where m is the mass of a particle and T is the system temperature. The time dependence of the mean-square displacement over the complete time range can be approximated by [19]

$$\sigma^2 = \frac{v^2t^2}{1+\dfrac{v^2}{2d}t^{2-2\mu}}. \tag{45}$$

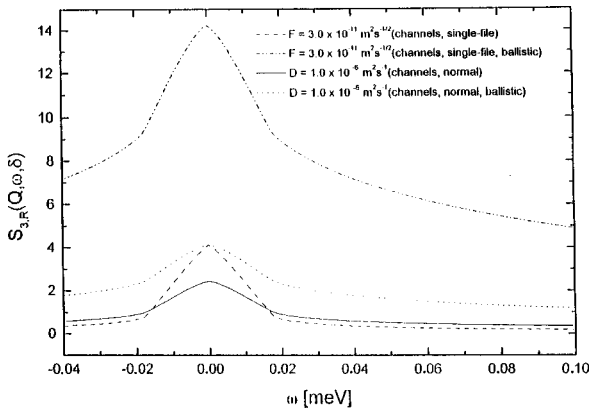

FIG. 12. The scattering function $S_{3,R}(Q,\omega,\delta)$ for three-dimensional normal diffusion and for normal and single-file diffusion with and without ballistic phase in isotropically oriented channels at $Q=0.35$ Å^{-1} (triangular resolution). Diffusivity and mobility chosen such that ranges influenced by ballistic phase and occupied by central peak overlap.

Inserting this approximation into Eq. (24), the scattering function and width for the case with ballistic behavior can be found. In the numerical calculations, a velocity $v=280$ m/s was used. This value corresponds to methane molecules at a temperature of $T=150$ K.

The consequences of the existence of a ballistic phase become obvious considering the transition times and the corresponding particles shifts. Figure 7 shows the space and time ranges (left and lower axes) together with the corresponding ranges of momentum and energy transfer (right and upper axis), which are relevant for quasielastic neutron scattering. The vertical straight line divides the plane into the range occupied by the central peak of the scattering function for the case without ballistic phase (right-hand side) and into the range not occupied by the central peak (left-hand side). The half width at the base of the central peak is assumed to be 2δ and the small dependence on Q is neglected. The mean shift σ for normal diffusion with initial ballistic phase together with the corresponding crossover times t_c is given for two diffusivities ($D=10^{-6}$ and 10^{-7} m^2/s). For the smaller diffusivity the crossover time is far away from the range occupied by the central peak and, therefore, the central peak should not be modified by the influence of the ballistic phase. With increasing diffusivity the range influenced by the ballistic phase grows towards the upper right corner. At $D\approx10^{-6}$ m^2/s the range influenced by the ballistic phase begins to overlap with the region occupied by the central peak of the scattering function. A change in the pattern of the scattering function and of the width should be expected in the case of such an overlap, i.e., in the present case for diffusivities larger than $D\approx10^{-6}$ m^2/s.

In Fig. 8, the FWHM for normal diffusion and triangular resolution with an initial ballistic phase in isotropically oriented channels is given. As expected from the interpretation of Fig. 7, for diffusivities $D<10^{-7}$ m^2/s the behavior of the FWHM is very similar to the case without an initial ballistic phase (see Fig. 2), whereas for a diffusivity of $D=10^{-6}$ m^2/s the behavior changes. In fact, the change in the behavior is dramatic and the FWHM increases rapidly instead of approaching a constant value for large Q. In all experimental cases studied so far, D is of the order of $D=10^{-9}$ m^2/s, and, therefore, the ballistic phase can be neglected.

In the case of single-file diffusion the situation is similar. In Fig. 9 the range influenced by the ballistic phase and the range occupied by the central peak of the scattering function are given for single-file diffusion. For single-file diffusion the overlap begins at a mobility of $F\approx2\times10^{-12}$ $m^2/s^{1/2}$. Again, when the two regions overlap, a significant change in the behavior of the FWHM is to be expected.

The FWHM for different mobilities F is given in Fig. 10. For mobilities smaller than 2×10^{-12} $m^2\,s^{-1/2}$ the influence of the ballistic phase is small (see Fig. 3) and the FWHM approaches a constant value for large Q. Otherwise, for mobilities larger than the above value, the widths are rapidly increasing with Q.

The strong increase of the FWHM can be understood by interpreting Fig. 1. In the ballistic phase the exponent of the time behavior [Eq. (32)] is $\mu=1$ and for this value the FWHM increases to infinity for large Q (see Fig. 1). Therefore, a stronger increase of the FWHM should be expected compared with the case without ballistic phase.

In PFG-NMR measurements, where the observed time scale is 1–100 ms and, therefore, the ballistic phase cannot be seen, mobilities of an order of $F=10^{-11}$ $m^2/s^{1/2}$ were found [7]. The mobility factor obtained from QENS for methane, $F=2\times10^{-12}$ $m^2/s^{1/2}$ corresponds to the limit where this effect has to be considered. Thus, measuring such systems by quasielastic neutron scattering, the analysis of the ballistic phase is necessary for the interpretation of the experimental results.

In Fig. 11 the scattering functions for $Q=0.35$ $Å^{-1}$ with and without ballistic phase are compared for a medium diffusivity and mobility. As to be expected from the interpretation of Fig. 7, the change of the scattering function is very small for normal diffusion with a diffusion coefficient of $D=10^{-8}$ $m^2\,s^{-1}$. In the case of single-file diffusion with a mobility of $F=4.1\times10^{-13}$ $m^2\,s^{-1/2}$, the scattering function with ballistic phase is larger than without. The main effect is in the wings outside of the central peak.

The scattering functions for a diffusivity or mobility, where a large change in the behavior is expected, are given in Fig. 12. Both for single-file and normal diffusion, the scattering functions are much larger than in the case without ballistic phase. The increase of the scattering functions outside the central peak is very strong leading to large widths as already seen in Figs. 8 and 10.

Reanalyzing the experimental data shown in Fig. 6 we have found that the diffusivity is small enough to justify the exclusion of a ballistic phase and hence of the possibility of a misinterpretation of the data by neglecting this effect. This result is in agreement with the above statement that the influence of the ballistic phase becomes negligible for diffusivities smaller than 10^{-6} $m^2\,s^{-1}$.

IX. SUMMARY

The phenomenon of single-file diffusion may be investigated by means of quasielastic neutron scattering. For diffusivities and mobilities large enough to lead to a significant broadening, diffusion in isotropically oriented one-dimensional channels can be well distinguished from three-dimensional normal diffusion. Furthermore, normal and single-file diffusion in such channels can also be distinguished and the determination of the diffusivity or mobility is possible. Due to the discontinuity of the self-correlation function $G_3(\mathbf{r},t)$ at $r=0$, the scattering function $S_3(\mathbf{Q},\omega)$ has a discontinuity at $\omega=0$ and the scattering function $S_{3,R}(\mathbf{Q},\omega,\delta)$ convoluted with the resolution function is much narrower than in the case of three-dimensional normal diffusion. Therefore, the resolution of the spectrometer used must be adapted accordingly.

In contrast to the case of three-dimensional normal diffusion where the FWHM increases linearly with the momentum transfer Q, the FWHM for diffusion in one-dimensional channels approaches a constant value at large Q, when the mean-square displacement is assumed to follow a power law (Eq. 32) over the full time range. For large diffusivities or mobilities the FWHM reaches its maximum value already at small momentum transfer ($Q<0.2$ $Å^{-1}$). On the other hand, for large diffusivities or mobilities the ballistic phase

describing the free motion of the particles at short times becomes essential. The influence of the ballistic phase leads to a significant increase of both the maximum of the scattering function and the FWHM. The behavior of the FWHM can change completely: instead of approaching a constant value at large Q, the FWHM increases over the full experimentally accessible range of the momentum transfer. Therefore, for the interpretation of experimental results, the influence of the ballistic phase should be taken into consideration, especially if a large diffusivity or mobility is expected.

ACKNOWLEDGMENT

This work was supported by Sonderforschungsbereich 294 of the Deutsche Forschungsgemeinschaft and by the European Community within The Joule Project No. JOE3-CT95-0018.

[1] P. A. Fedders, Phys. Rev. B **17**, 40 (1978).
[2] J. Kärger, Phys. Rev. A **45**, 4173 (1992); Phys. Rev. E **47**, 1427 (1993).
[3] K. Hahn and J. Kärger, J. Phys. A **28**, 3061 (1995).
[4] H. van Beijeren, K. W. Kehr, and R. Kutner, Phys. Rev. B **28**, 5711 (1983).
[5] J. Kärger, M. Petzold, H. Pfeifer, S. Ernst, and J. Weitkamp, J. Catal. **136**, 283 (1992).
[6] K. Hahn and J. Kärger, J. Phys. Chem. **100**, 100 (1996).
[7] K. Hahn, J. Kärger, and V. Kukla, Phys. Rev. Lett. **76**, 2762 (1996).
[8] V. Gupta, S. S. Nivarthi, A. V. McCormick, and H. T. Davis, Chem. Phys. Lett. **247**, 596 (1995).
[9] H. Jobic, K. Hahn, J. Kärger, M. Bée, A. Tuel, M. Noack, I. Girnus, and G. J. Kearley, J. Phys. Chem. **101**, 5834 (1997).
[10] J. Kärger and D. M. Ruthven, *Diffusion in Zeolites and Other Microporous Solids* (Wiley, New York, 1992).
[11] M. Eic and D. M. Ruthven, Zeolites **8**, 472 (1988); D. M. Ruthven and M. Eic, Am. Inst. Chem. Eng. Symp. Ser. **368**, 302 (1988).
[12] L. V. C. Rees, in *Proceedings of the 10th International Zeolite Conference, Garmisch-Partenkirchen, 1994*, edited by J. Weitkamp, H. G. Karge, H. Pfeifer, and W. Hölderich (Elsevier, Amsterdam, 1994).
[13] M. Ylihautala, J. Jokisaari, E. Fischer, and R. Kimmich, Phys. Rev. E **57**, 6844 (1998).
[14] H. Jobic, in *Catalyst Characterization: Physical Techniques for Solid Materials*, edited by B. Imelik and J. C. Vedrine (Plenum Press, New York, 1994), p. 347.
[15] M. Bée, *Quasi-elastic Neutron Scattering* (Adam Hilger, Bristol, 1988).
[16] H. Jobic, M. Bée, and A. Renouprez, Surf. Sci. **140**, 307 (1984).
[17] A. P. Prudnikov, J. A. Brychkov, and I. O. Marichev, *Integrals and Series* (Nauka, Moscow, 1981).
[18] *Handbook of Mathematical Functions*, edited by M. Abramowitz and I. A. Stegun (Dover Publications, New York, 1968).
[19] S. Brandani, J. Catal. **160**, 326 (1996); J. Kärger and K. Hahn, *ibid.* **160**, 328 (1996).